

Effects of substitution for Cu in CuO_2 planes with dopants of different electron configuration in $\text{YBa}_2\text{Cu}_3\text{O}_7$

This article has been downloaded from IOPscience. Please scroll down to see the full text article.

1993 J. Phys.: Condens. Matter 5 3623

(<http://iopscience.iop.org/0953-8984/5/22/013>)

View [the table of contents for this issue](#), or go to the [journal homepage](#) for more

Download details:

IP Address: 171.66.16.96

The article was downloaded on 11/05/2010 at 01:22

Please note that [terms and conditions apply](#).

Effects of substitution for Cu in CuO_2 planes with dopants of different electron configuration in $\text{YBa}_2\text{Cu}_3\text{O}_7$

Y Zhao†, H K Liu, G Yang and S X Dou

School of Materials Science and Engineering, University of New South Wales, PO Box 1, Kensington, NSW 2033, Australia

Received 29 June 1992, in final form 27 January 1993

Abstract. The effects of substitution for copper in the system $\text{YBa}_2\text{Cu}_{3-x}\text{M}_x\text{O}_{7-y}$, with $\text{M}=\text{Ni}$, Zn and $\text{Ni}_{1/2}\text{Zn}_{1/2}$, and $0 \leq x \leq 0.5$, have been studied with respect to its superconducting transition temperature, hole concentration, electronic transport properties in the normal state and structure parameters. The results strongly indicate that the band filling, the excess of holes, and electron localization due to the destruction of the integrity of the CuO_2 planes are not the predominant factors for the suppression of T_c in the case of substitution for $\text{Cu}(2)$. Semi-quantitative analyses reveal that the Zn and Ni ions act as impurity scattering centres with a radius of scattering cross larger than the average Cu–O bond length of the CuO_2 planes, which directly destroys the superconducting path in CuO_2 planes and decreases the superconducting energy gap. This may be the main reason for the suppression of superconductivity.

1. Introduction

The substitution of different atoms in the high-temperature superconductor Y-123 is an important method for obtaining essential information about superconductivity. The mechanism of the suppression of T_c by substituting Y, Ba and Cu(1) (the copper atom at the chain site) can be well explained by hole filling and/or changes of charge carrier concentration. For example, the substitution of Al^{3+} , Co^{3+} and Ga^{3+} for Cu(1) reduces the hole concentration, and substituting La for Ba also has a similar effect [1–6]. The effect of this kind of substitution, which reduces the hole concentration, on superconductivity and hole concentration can be counterbalanced, to various degrees, by the simultaneous replacement of Y with Ca, since the substitution of Ca for Y increases the hole concentration. In this way, T_c can, to some extent, be restored [7, 8]. However, no consistent picture has yet been evolved to explain the mechanism causing the suppression of T_c by substituting for Cu(2) (copper in the CuO_2 planes), which is found to be one of the highest rates of T_c suppression for element substitution in high- T_c superconductors. Some mechanisms such as band filling and hole overdoping [9, 10] have been proposed, but they are being sharply challenged by more and more experimental results, for example from x-ray absorption and spectroscopic polarization modulation ellipsometric spectra [11, 12], specific heat measurements [13, 14], and the Hall effect [15]. It seems that the effect of electron localization induced by the destruction of the integrity of the CuO_2 planes is a common feature existing in high-temperature superconductors [16, 17], whether it is the real reason for the suppression of T_c especially in this case, is still an open question.

† Department of Physics, Zhejiang University Hangzhou, Zhejiang, 310027 People's Republic of China.

As regards the site occupied by Zn and Ni, earlier neutron scattering experiments suggested that Zn is located at the chain position Cu(1), but more accurate neutron diffraction results [18, 19] indicate that Ni and Zn definitely occupy the plane site Cu(2). Our experiment is based on this conclusion. Since Zn^{2+} has a filled 3d shell ($3d^{10}$) while Ni^{2+} has the electron configuration $3d^8$, $(\text{Zn}, \text{Ni})^{2+}$ has a mixture of $3d^{10}$ and $3d^8$. As the dopants have different electron configurations, they might have different influences on the electron properties, superconductivity, etc. In this paper we present the measurements of superconductivity, hole concentration, electrical resistivity and lattice parameters for $\text{YBa}_2\text{Cu}_{3-x}\text{M}_x\text{O}_{7-y}$ with $M=\text{Ni}, \text{Zn}$ and $\text{Ni}_{1/2}\text{Zn}_{1/2}$. The results strongly support the theory that instead of band filling, hole overdoping and electron localization, the destruction of the superconducting path in CuO_2 planes, as well as the decrease in the superconducting energy gap, may be the main reasons for the suppression of T_c in the case of substitution for copper in the CuO_2 planes.

2. Experimental details

A series of samples with composition $\text{YBa}_2\text{Cu}_{3-x}\text{M}_x\text{O}_{7-y}$ ($M=\text{Ni}, \text{Zn}$ and $\text{Ni}_{1/2}\text{Zn}_{1/2}$, and $0 \leq x \leq 0.5$) were prepared by mixing Y_2O_3 , BaCO_3 , CuO , ZnO and NiO powders in stoichiometric proportions and firing in air at 900°C for 20 h. The powders were reground and reheated at 920°C for 24 h. This processing was repeated several times with the firing temperature successively raised by 5°C each time in order to obtain more homogeneous and sufficiently reacted samples. Finally the powders were pressed into pellets, sintered in air at 930°C for 20 h, then cooled to room temperature in the oven. The post-heat treatment was carried out in flowing oxygen at 920°C for 30 h, then the samples were cooled to 600°C , and soaked for 20 h, and finally cooled to room temperature at a rate of 50°C h^{-1} . Microstructural and compositional analysis were performed with a JEOL JSM840 scanning electron microscope (SEM) equipped with a Link System AN 10000 energy dispersive spectrometer (EDS) and x-ray powder diffraction patterns were obtained with a Siemens Diffractometer D5000 using $\text{CuK}\alpha$ radiation. All samples were carefully characterized by x-ray diffraction, SEM and EDS analyses and confirmed to be single phase. Some typical x-ray diffraction patterns are shown in figure 1, which demonstrates that the samples are good single-phase. The results of the EDS analyses for the samples are given in table 1. It is evident that both Ni and Zn have been introduced into the lattice. In contrast to the results reported by other groups [20, 21], our samples have compositions very close to their nominal ones, indicating that long-term heating aids the dissolving of the M^{2+} ions into the CuO_2 planes. On the basis of the conclusions that both the Zn^{2+} and Ni^{2+} occupy the Cu(2) site [18, 19], we believe that in our samples the Ni and Zn occupy the Cu(2) site. As regards the microstructure of the samples, no distinct difference can be seen between the samples with $x \leq 0.20$. However, as x is greater than 0.25, the grain size becomes smaller with the increase of the dopant content (see figure 2). Oxygen content of the samples was determined by the volumetric method [22]. Resistivity of the samples was measured with the DC 4-probe technique. AC susceptibility measurements were used to determine the superconducting critical temperature of the samples. All of the T_c values given in this paper are corresponding to the onset transition of the AC susceptibility measurements, which are consistent with those determined from resistivity measurements.

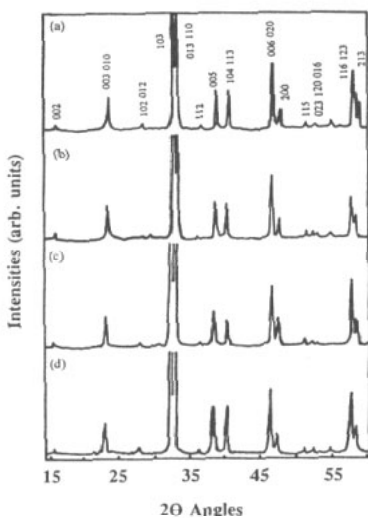


Figure 1. Typical x-ray diffraction patterns of YBa₂Cu_{3-x}M_xO₇ systems with M=Zn, Ni and Zn_{1/2}Ni_{1/2}. (a) $x = 0$, (b) $x = 0.1$, M=Zn, (c) $x = 0.1$, M=Zn_{1/2}Ni_{1/2} and (d) $x = 0.25$, M=Zn_{1/2}Ni_{1/2}.

Table 1. The EDS analyses of YBa₂Cu_{3-x}(Ni_{1/2}Zn_{1/2})_xO_{7-y} systems.

x	Y	Ba	Cu	Ni	Zn
0	1.40	1.95	0.91	0.00	0.00
0.05	1.37	1.98	2.89	0.02	0.02
0.10	1.37	2.00	2.83	0.05	0.08
0.20	1.37	1.96	2.80	0.10	0.11
0.30	1.49	2.00	2.45	0.11	0.13
0.40	1.41	2.01	2.53	0.17	0.18
0.50	1.35	2.18	2.37	0.20	0.23

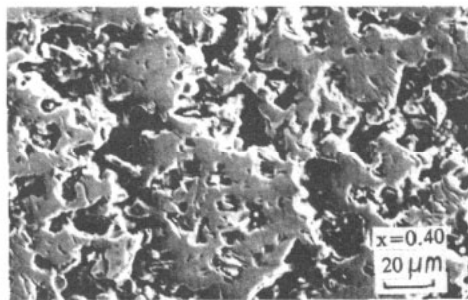
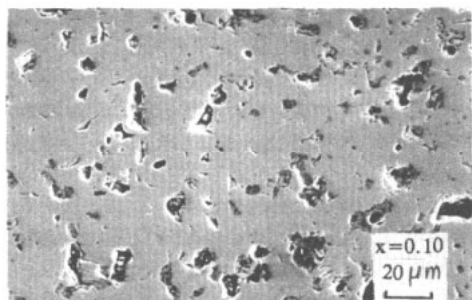


Figure 2. The microstructure of some YBa₂Cu_{3-x}(Zn_{1/2}Ni_{1/2})_xO₇ samples.

3. Experimental results

Figure 3 shows the variations of the lattice parameters with the dopant content x of the YBa₂Cu_{3-x}M_xO_{7-y} system. For the different kinds of dopant, the samples remain

orthorhombic throughout the whole composition range up to $x = 0.5$, indicating that the Zn and Ni only substitute for Cu atoms in the CuO_2 planes. It can also be seen that the lattice parameters a , b and c change very little for different dopants and in different doping levels. This means that Zn and Ni substitution for Cu(2) merely very slightly modifies the bond lengths between the atoms in the system.

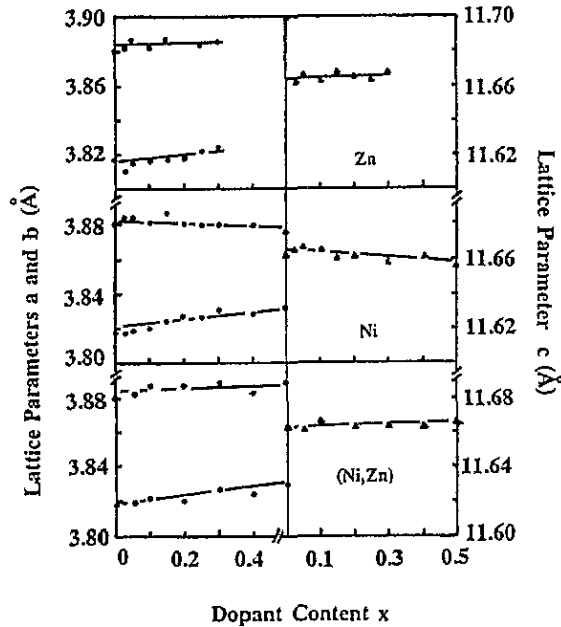


Figure 3. Variations of lattice parameters a , b and c with dopant content x in the $\text{YBa}_2\text{Cu}_{3-x}\text{M}_x\text{O}_7$ system with $\text{M}=\text{Zn}$, Ni and $\text{Zn}_{1/2}\text{Ni}_{1/2}$.

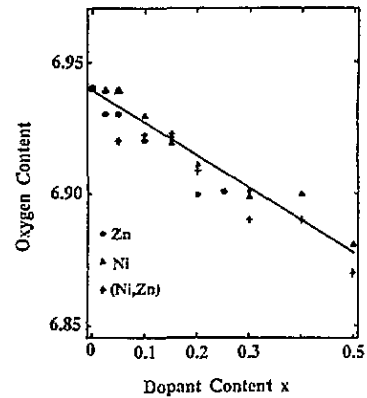


Figure 4. Relationship between oxygen content and dopant content x in the $\text{YBa}_2\text{Cu}_{3-x}\text{M}_x\text{O}_7$ system with $\text{M}=\text{Zn}$, Ni and $\text{Zn}_{1/2}\text{Ni}_{1/2}$.

Figure 4 shows the variation of the oxygen stoichiometry with dopant content for $\text{YBa}_2\text{Cu}_{3-x}\text{M}_x\text{O}_{7-y}$. Though all samples have been annealed in a pure oxygen atmosphere for a long time, the oxygen content decreases systematically from 6.94 to 6.87 as the dopant content changes from 0 to 0.5. The trends in the changes of the oxygen stoichiometry with the dopant content are almost the same in the three doped systems. It is therefore evident that the influences of Zn and Ni on the crystal structure and the charge balance of the Y-123 system are quite similar.

The results of AC susceptibility measurements for different samples are shown in figure 5. It is evident that all doped samples have lower values of T_c than the undoped Y-123 sample. With increase of dopant content, T_c gradually decreases and the transition width becomes larger. This is a common feature of a doped system. Figure 6 shows the variation of T_c with dopant content x . It is seen that T_c decreases with x for various dopants, but the rates of decrease are quite different, depending on the different doping elements. The highest rate of T_c suppression is for $\text{M}=\text{Zn}$, with $dT_c/dx = 9.1 \text{ K/at.}\%$, this value is consistent with the results of other authors for polycrystalline samples [23], but smaller than that observed in a crystal film [24]. The latter has a higher rate of $10.3 \text{ K/at.}\%$. This may be due to the more homogeneous distribution of the dopants in a crystal film than in polycrystalline samples. The second highest rate is for $\text{M}=\text{Zn}_{1/2}\text{Ni}_{1/2}$, with $dT_c/dx = 7.3 \text{ K/at.}\%$. The

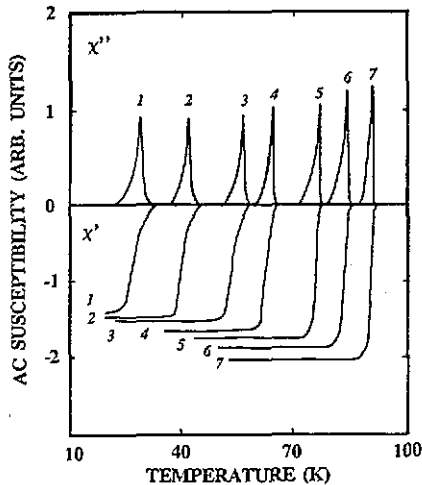


Figure 5. AC susceptibility of the $\text{YBa}_2\text{Cu}_{3-x}\text{M}_x\text{O}_7$ systems with compositions 1 $\text{M}=\text{Zn}$, $x = 0.2$, 2 $\text{M}=\text{Zn}_{1/2}\text{Ni}_{1/2}$, $x = 0.2$, 3 $\text{M}=\text{Zn}$, $x = 0.1$, 4 $\text{M}=\text{Zn}_{1/2}\text{Ni}_{1/2}$, $x = 0.1$, 5 $\text{M}=\text{Zn}_{1/2}\text{Ni}_{1/2}$, $x = 0.05$, 6 $\text{M}=\text{Ni}$, $x = 0.05$, 7 $x = 0$.

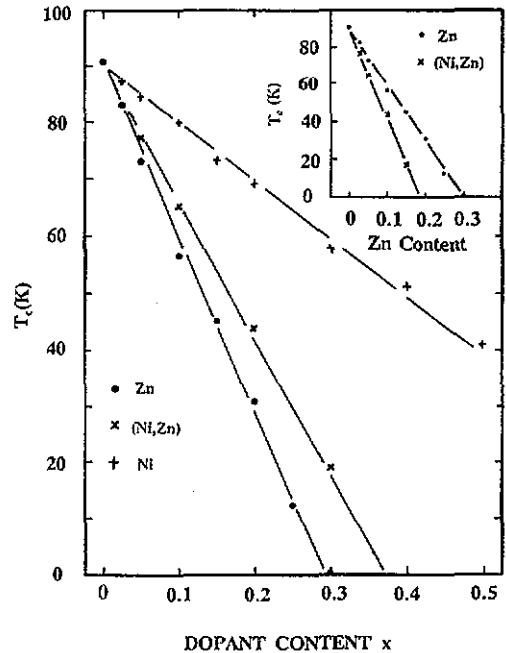


Figure 6. Variation of T_c with dopant content of $\text{YBa}_2\text{Cu}_{3-x}\text{M}_x\text{O}_7$ systems with $\text{M}=\text{Zn}$, Ni , and $\text{Zn}_{1/2}\text{Ni}_{1/2}$. The inset is the comparison in T_c between $\text{YBa}_2\text{Cu}_{3-x}\text{Zn}_x\text{O}_{7-y}$ and $\text{YBa}_2\text{Cu}_{3-x}(\text{Zn}_{1/2}\text{Ni}_{1/2})_x\text{O}_{7-y}$ systems with the same Zn content.

least significant influence on T_c is observed in the case $\text{M}=\text{Ni}$, where the dT_c/dx is merely 3.0 K/at. %.

The electrical resistivity of the $\text{YBa}_2\text{Cu}_{3-x}\text{M}_x\text{O}_{7-y}$ samples with $\text{M}=\text{Zn}$, Ni , and $\text{Ni}_{1/2}\text{Zn}_{1/2}$ are shown in figure 7. The resistivity of the samples increases with dopant content in all cases. At lower dopant content ($x \leq 0.2$), the resistivity increases linearly with x ; but as x becomes larger than 0.2, the resistivity goes up with the dopant content more rapidly than the linear relation (see figure 8). There are several factors that may lead to the increase of resistivity with dopant content. The first is a modification of the electronic structure, for example, a shift of Fermi energy, which can change the carrier concentration and consequently the resistivity. The second is the impurity scattering effect caused by the dopants. Besides these intrinsic properties, there are some extrinsic factors that can also result in an increase of resistivity, a typical one being the grain-boundary effect. According to our results on the microstructural analyses, the morphology and grain size for samples with a lower doping level ($x \leq 0.2$) are almost the same. Therefore the grain-boundary effect should be nearly the same in these samples, and the variation of the resistivity with the doping level should be mainly controlled by the intrinsic modification of the electronic states. For samples with a higher doping level ($x > 0.25$), the grain size becomes smaller and smaller with increasing doping level, and the morphology of the microstructure is also modified by the doping process. Thus it can be believed that in this case, the grain-boundary effect may become more and more pronounced with increasing doping level, and the variation of the resistivity with doping level can be controlled by both intrinsic and extrinsic modifications. This may be one of the reasons why the resistivity

increases with doping level more rapidly with $x \leq 0.2$ than with $x > 0.25$ (see also the figure 8). The temperature coefficient of resistivity (TCR) changes from positive to negative at $x > 0.3$ for the Zn-doped system, and at $x > 0.4$ for the $\text{Ni}_{1/2}\text{Zn}_{1/2}$ -doped system. For the Ni-doped system, the TCR remains positive in the whole range of the composition studied.

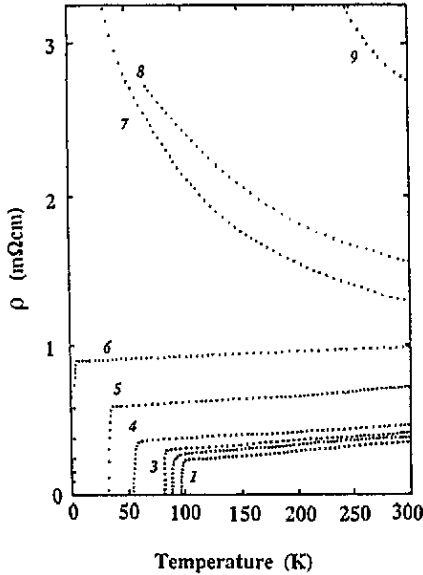


Figure 7. The temperature dependence of resistivity of $\text{YBa}_2\text{Cu}_{3-x}\text{M}_x\text{O}_{7-y}$ systems with composition l $x = 0$, 2 $\text{M}=\text{Ni}$, $x = 0.05$, 3 $\text{M}=\text{Ni}$, $x = 0.1$, 4 $\text{M}=\text{Zn}$, $x = 0.1$, 5 $\text{M}=\text{Zn}$, $x = 0.2$, 6 $\text{M}=\text{Zn}$, $x = 0.3$, 7 $\text{M}=\text{Zn}$, $x = 0.35$, 8 $\text{M}=\text{Zn}_{1/2}\text{Ni}_{1/2}$, $x = 0.4$, 9 $\text{M}=\text{Zn}_{1/2}\text{Ni}_{1/2}$, $x = 0.5$.

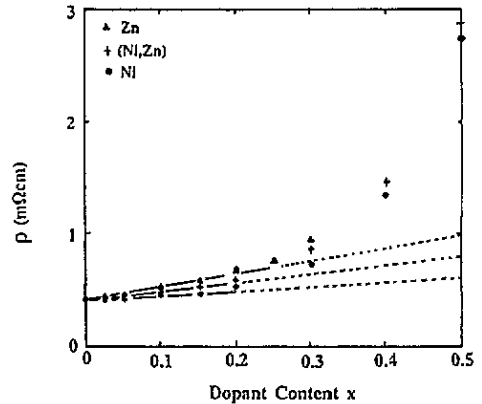


Figure 8. Variation of normal state resistivity with dopant content x in the $\text{YBa}_2\text{Cu}_{3-x}\text{M}_x\text{O}_7$ system.

Figure 9 shows the residual resistivity of the sample, which is obtained by extrapolating the data to the zero temperature. It can be seen that the residual resistivity is proportional to the dopant content for these doped systems, indicating that the Zn and Ni atoms act as independent impurity scattering centres. The slope of the residual resistivity against dopant content varies with different dopants. The Zn-doped system has the greatest slope and the Ni-doped system has the smallest. This indicates that Zn has a larger scattering cross section than Ni.

4. Discussion

It is interesting to note from figure 6 that the smallest rate of T_c suppression is not for $\text{M}=\text{Ni}_{1/2}\text{Zn}_{1/2}$ but for $\text{M}=\text{Ni}$. Based on the electron band picture, a Zn^{2+} ion with a filled 3d shell will provide an extra electron for the Cu shell when it occupies the Cu(2) site and consequently fills the antibonding dx^2-y^2 band. This was regarded as the reason for the lowering of T_c [3, 4]. If this argument is tenable, the simultaneous substitution of Ni for Cu(2) would counterbalance the effect of the substitution of Zn for Cu(2) because Ni^{2+}

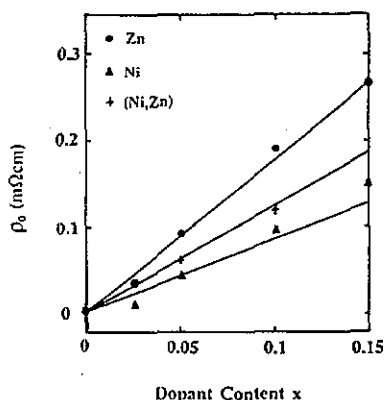


Figure 9. The relationship between the residual resistivity and dopant content of YBa₂Cu_{3-x}Ni_xM_xO₇ systems with M=Zn, Ni, and Zn_{1/2}Ni_{1/2}.

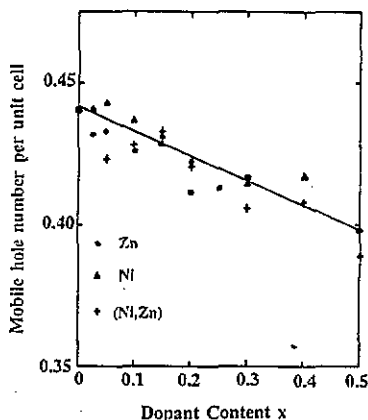


Figure 10. The variation of mobile hole concentration with dopant content in YBa₂Cu_{3-x}M_xO₇ systems with M=Zn, Ni, and Zn_{1/2}Ni_{1/2}. A good linear relationship between them can be seen.

has the electron configuration of 3d⁸ which will provide an extra hole for the Cu shell when it occupies the Cu(2) site, and consequently compensate the extra electron added by Zn. As a result, T_c would be redeemed to some extent, but this is not in fact the case. As shown in the inset of figure 6, corresponding to the same content of zinc, the Zn–Ni co-substituted samples have lower T_c indicating that the simultaneous substitution of Ni is unable to counterbalance the effect of Zn substitution on T_c , on the contrary, it enhances the suppression of T_c . This hints that the hole filling is not the reason for the suppression of T_c by Zn substitution for Cu(2). In order to further understand this point, we should analyse the changes of the hole concentration of these doped systems.

It is generally believed that the hole concentration is associated with the oxygen content as well as the doping level in the YBa₂Cu₃O_{7- δ} system [7, 8]. In the case of substitution for Cu(2), since Zn and Ni have a slight influence on the crystal structure, as shown in figure 3 and the charge balance between the CuO₂ plane and the Cu–O chain is not affected, as shown by Raman spectrum studies [24–26], the oxidation state of copper as well as the hole concentration will not be modified much by Zn and Ni substitution. However, the number of Cu atoms in the CuO₂ plane is reduced by substituting them by Cu(2), which will slightly reduce the mobile hole concentration of the system by a factor of (2 – x). By using a formula similar to those given in reference [8], after considering the reduction of the number of Cu(2) atoms, we can estimate the mobile hole concentration as follows. For the doped system YBa₂Cu(1)Cu(2)_{2-x}M_xO_{7-y}, the total mobile hole number per unit cell, n_p , can be described as

$$n_p = (2 - x)P_{sh} \quad (1)$$

where the factor (2 – x) represents the number of Cu(2) atoms in the unit cell. P_{sh} is the mobile hole number per Cu in the CuO₂ planes, which obeys the following relations

$$3P = 2P_{sh} + P_c \quad (2a)$$

$$P_c = 0.5 - y \quad (2b)$$

in which the P_c is the localized hole number per Cu in the CuO chains and P is the average hole number per Cu of the unit cell, which is determined by the charge balance conditions.

In the present case, it can be described as

$$P = (1 - 2y)/(3 - x). \quad (3)$$

The results of the mobile hole concentration determined as mentioned above are shown in figure 10. It can be clearly seen that for the three doped systems, the mobile hole concentration, n_p , decreases linearly with dopant content in the same way, which illustrates that Zn and Ni play the same role in the concentration of the holes although their electronic configurations are very different, i.e. both the Zn and Ni substitution for Cu(2) slightly reduce the hole concentration by reducing the number of Cu(2) instead of by the band filling effect. This precludes the hole overdoping and band filling as the explanation for the T_c suppression in Zn- and Ni-doped system. It is because of this that the effect of Zn substitution for Cu(2) cannot be counterbalanced by further substituting Ni and vice versa. It may also be the reason why the effect of Zn substitution for Cu(2) cannot be counterbalanced by the simultaneous substitution of other elements, as we have previously observed [27].

As we know, in two-dimensional (2D) system, the Coulomb interaction effect is largely enhanced by the disorder [28]. Within the mean-field approximation it has shown that T_c is decreased by increasing sheet resistance due to an increase in the Coulomb interaction. Does this localization effect play a significant role for the depression of T_c in the present systems? If it is the case, the relationship between T_c and the disorder (represented by the resistivity) should obey the following equation [29]

$$\ln[T/T_{c0}] = -\{(g_1 - 3g')N(0)/4\pi\epsilon_F\tau_0\}[\ln(1/\tau_0 T_c)]^2 - \{(g_1 + g')N(0)/4\pi\epsilon_F\tau_0\}[\ln(1/\tau_0 T_c)]^3 \quad (4)$$

where T_{c0} is the transition temperature in the pure system, $R = \pi/e^2\epsilon_F\tau_0$ is the sheet resistance, g_1 and g' are the Coulomb interaction and attractive interaction respectively, $N(0)$ is the state density of electrons at the Fermi level, and $1/\tau_0$ is the rate of scatter of an electron. In terms of the superconducting coherence length of the pure system and the mean free path of an electron, $\xi_0 = v_F/1.75\pi T_{c0}$ and $l = v_F\tau_0$ (v_F is the Fermi velocity) respectively. $1/\tau_0$ can be expressed as $1/\tau_0 = 5.5\xi_0 T_{c0}/l$.

In order to compare the experimental data with the theory, we take the normal state resistivity to be approximately the sheet resistance multiplied by a constant factor, i.e. $R = \beta\rho$, where β is an adjustable constant depending on the peculiarities of the system, such as the anisotropy, grain alignment and the microstructure for the polycrystalline samples. Figure 11 shows the relationship between T_c and ρ for our samples and a comparison with the theoretical results based on equation (4). It is evident that the experimental data cannot be fitted by the equation although the parameter $1/\tau_0 T_{c0}$ has been changed over a wide range. In our opinion, there are at least two main factors which may give rise to the disagreement between the experimental data and the theoretical results of equation (4). First of all, it the T_c suppression is not caused by the localization effect, the T_c - ρ relation will, of course, not obey equation (4). In other words, the disagreement shown in figure 11 suggests that the electron localization is not the main cause of the T_c suppression. Secondly, if $\text{YBa}_2\text{Cu}_3\text{O}_{7-y}$ is not a strong 2D system, equation (4) could not properly describe the variation of T_c with resistivity, and thus it is easy to understand the disagreement between the theoretical and experimental results. However, it should be pointed out that the superconducting coherence length along the c axis in $\text{YBa}_2\text{Cu}_3\text{O}_{7-y}$ is merely 1.5–3 Å [30], which is much shorter than 8.2 Å, the distance from a pair of two immediately adjacent CuO_2 planes to the next pair.

This suggests that the superconducting coupling along the c axis is extremely weak, and the superconductivity is mainly along the CuO_2 planes. In the normal state, the resistivity along the c axis is at least ten times greater than that along the ab plane [30]. All these factors mean that $\text{YBa}_2\text{Cu}_3\text{O}_{7-y}$ is highly anisotropic both in superconducting and normal states and thus it is quite possible to deal with it as a 2D system. In fact, it has been observed that in the Fe-doped $\text{YBa}_2\text{Cu}_3\text{O}_{7-y}$ system the relationship between T_c and ρ can be well fitted by equation (4) [31], indicating that $\text{YBa}_2\text{Cu}_3\text{O}_{7-y}$ can be dealt with as a 2D system. therefore, it is reasonable to believe that the disagreement between the experimental and theoretical results in figure 11 mainly originates from some kind of non-localization effect caused by doping Zn or Ni instead of from other factors.

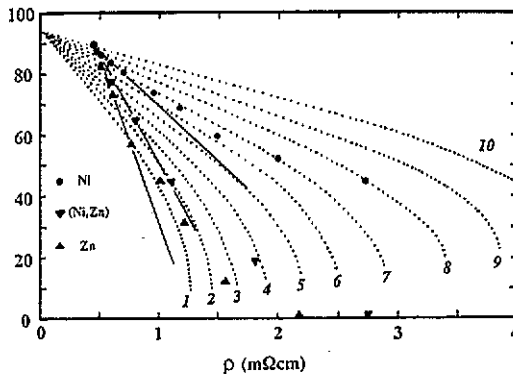


Figure 11. The relationship between T_c and normal state resistivity for $\text{YBa}_2\text{Cu}_{3-x}\text{M}_x\text{O}_7$ systems with $M=\text{Zn}$, Ni , and $\text{Zn}_{1/2}\text{Ni}_{1/2}$. The dotted curves represent the calculation from the Meakawa-Fukuyama theory (see equation (4)) with parameters $1/\tau_0 T_{c0}$ of: 1 70, 2 60, 3 50, 4 40, 5 30, 6 25, 7 20, 8 15, 9 12.5 and 10 10. The solid lines represent the experimental results. A remarkable crossover can be seen for each of the full lines with theoretical curves of different $1/\tau_0 T_{c0}$ values.

In order to understand the deviation of the T_c - ρ relation obtained experimentally from that determined by equation (4), it is worth noting that the trends of T_c with ρ (see the full lines of figure 11) show a remarkable crossover, for all three systems, with the theoretical curves of various values of $1/\tau_0 T_{c0}$. For the Zn-doped system, for example, the trend of T_c with ρ starts from the curve corresponding to $1/\tau_0 T_{c0} = 10$; with increasing resistivity, it does not keep going along this curve but crosses to another curve with a different value of $1/\tau_0 T_{c0}$. At $\rho = 1.26 \text{ m}\Omega \text{ cm}$, it reaches the curve with $1/\tau_0 T_{c0} = 70$. Similar behaviour has been observed for Ni- and $(\text{Ni}_{1/2}\text{Zn}_{1/2})$ -doped $\text{YBa}_2\text{Cu}_3\text{O}_{7-y}$, but the magnitude of the deviation of the T_c - ρ relationship obtained experimentally from that determined by equation (4) becomes smaller and smaller as M^{2+} changes from Zn^{2+} to Ni^{2+} . The increase of $1/\tau_0 T_{c0}$ means that either τ_0 or T_{c0} is decreased. The former suggests an enhancement of the scattering for the electrons, the latter suggests a decrease of the superconducting energy gap, $\Delta(0)$, since $\Delta(0)$ is proportional to T_{c0} . Both of the possibilities may exist in the system, and, as we will analyse below, they are closely related.

Now we examine the modification of electron scattering, induced by doping with Zn or Ni, by examining the electronic transport properties. Although the experimental results of the resistivity measurements on polycrystalline samples is somewhat complicated, the results can still be regarded approximately as the resistivity in ab -plane since the current

flows along paths of least resistance. On the basis of this viewpoint, the radius of scattering cross section caused by Zn or Ni can be estimated. As shown in figure 9, the residual resistivity ρ_0 increases linearly with x at the rate $d\rho_0/dx = 1.6 \text{ m}\Omega \text{ cm}$ for the Zn-doped system, $1.3 \text{ m}\Omega \text{ cm}$ for the (Zn, Ni)-doped system and $0.9 \text{ m}\Omega \text{ cm}$ for the Ni-doped system. For a 2D system, the resistivity due to s-wave scattering is $\Delta\rho_s = 4(h/2\pi e^2)(n_1/n) \sin^2 \delta_0$, where n_1 is the impurity concentration and δ_0 is the phase shift [32]. If we take $n = 0.225$ hole per Cu(2), the $\Delta\rho_s$ at the unitarity limit will be $730 \Omega \square^{-1}$ per 1% impurity. This means that each dopant presents a scattering cross section to the charge carriers of radius 5.0 \AA for Zn ions, and 3.8 \AA for Ni ions. These values are larger than those obtained by Chien *et al* [32]. The reason may be due to the additional scattering of the grain-boundaries in our polycrystalline samples. Therefore, our results clearly show that both Zn and Ni act as impurity scattering centres, which can explain why τ_0 is decreased by doping with Zn or Ni. In addition, our results also show that Zn induces a larger scattering cross section than Ni, which is in agreement with the fact that the crossover behaviour in the Zn-doped system is more pronounced than that in the Ni-doped system. On the other hand, since both Zn and Ni ions present a scattering cross section with a radius larger than the average Cu–O bond length (1.94 \AA) of the CuO_2 plane, a non-superconducting core may be induced around each Zn ion. As a result, the superconducting path in the CuO_2 will gradually be destroyed in a way similar to percolation. At the threshold of the percolation the superconductivity will be completely suppressed. The critical value of the dopant content corresponding to the percolation threshold will depend on the radius of the normal core, or the size of the scattering cross section. This may be the reason why the Zn ions suppress T_c more strongly than the Ni ions do. That is to say that the greater rate of T_c suppression caused by Zn than by Ni is due to the larger scattering cross section presented by Zn than by Ni, instead of the different band filling effect between them. Also, the occurrence of the normal core will result in a kind of pair-breaking effect as proposed theoretically [33], leading to a decrease of the superconducting energy gap and consequently the suppression of T_{c0} . This is also consistent with the crossover phenomenon shown in figure 11. Recently, Marsiglio [34] showed theoretically that for the attractive Hubbard model, the normal impurities, acting as magnetic impurities, are pair breaking for narrow bands. This theory is within the framework of the hole mechanism of superconductivity and in the strong-coupling limit can also be regarded as an explanation of the decrease of the superconducting energy gap in our samples since the high- T_c cuprates are typical systems with strong electron–electron correlation.

It should be pointed out that the analyses and discussion are merely from the point of view of the electronic properties of the system. As we know, the high- T_c superconductivity is closely related to the magnetic properties of the system. Apart from the modification of the electronic properties caused by Zn or Ni doping, the magnetic properties may have been modified as well. Whether the changes of the magnetic properties are more important than those of the electronic properties and what the intrinsic relation between them is are still questions to be answered. However, our results have shown, at least, that Zn or Ni ions doping in the CuO_2 planes directly affect the superconductivity.

5. Conclusion

In summary, the results and discussion given above show that the substitution of Zn or Ni for Cu(2) slightly decreases the mobile hole concentration through reducing the Cu(2) number other than by the band filling effect, which also precludes the hole overdoping

mechanism as an explanation of the T_c suppression. The relationship between T_c and resistivity (represents the disorder) cannot be fitted by the 2D disorder theory and a remarkable crossover phenomenon is presented, indicating that the electron localization due to the destruction of the integrity of the CuO₂ planes is not the predominant factor in the suppression of T_c . In fact, Zn or Ni ions act as impurity scattering centres with a radius of scattering cross section larger than the average Cu–O bond length of the CuO₂ planes, which directly destroys the superconducting path in the CuO₂ planes and decreases the superconducting energy gap.

Acknowledgments

The authors gratefully acknowledge the financial support of Metal Manufactures Ltd, the Commonwealth Department of Industry, Technology and Commerce, and the University of New South Wales. YZ is also grateful to The Fok Ying Tong Education Foundation for their support. Thanks are also given to Dr H Yamauchi (in ISTEC, Japan) for helpful discussions.

References

- [1] Tarascon J M, Barbour P, Miceli P F, Greene L H and Hull G W 1988 *Phys. Rev. B* **37** 7458
- [2] Clayhold J, Hagan S, Wang Z Z and Ony N P 1989 *Phys. Rev. B* **39** 777
- [3] Xiao G, Cieplak M Z, Gavrin A, Streitz F H, Bakhshai A and Chien C L 1988 *Phys. Rev. Lett.* **66** 1446
- [4] Matsuda A, Kinoshita K, Ishii T, Shibata H, Watanabe T and Yamada T 1988 *Phys. Rev. B* **38** 2910
- [5] Bazuev G V, Krylov K R, Ponomarev A I, Tsidilkovskii V I, Tsidilkovskii I M and Charikova T B 1989 *Phys. Status Solidi (a)* **115** 267
- [6] Cava R J, Batlogg B, Fleming R M, Sunshine S A, Ramirez A, Rietman E A, Zahurak S M and van Dover R B 1988 *Phys. Rev. B* **37** 5912
- [7] Zhao Y, Liu H K and Dou S X 1991 *Physica C* **179** 207
- [8] Tokura Y, Torrance J B, Huang T C and Nazzari A I 1988 *Phys. Rev. B* **38** 7156
- [9] Xiao G, Xiao J Q, Chien C L and Cieplak M Z 1991 *Phys. Rev. B* **43** 1245
- [10] Shafer M W, Penney T, Olsen B L, Greene R L and Kock R H 1989 *Phys. Rev. B* **39** 2914
- [11] Rao R V R, Singhal R K, Jain D C, Chandka U, Chauhan H S, Saini N L, Gray K B, Rao C V N I, Agarwal S K and Narlikar A V 1978 *Mod. Phys. Lett. B* **3** 1157
- [12] Sengupta L C, Roughani B, Auel J L, Sundaram S and Joiner W C H 1991 *Physica C* **175** 17
- [13] Meingast C, Ahrens R, Blank B, Burkle H, Rudolf B and Wuhl H 1991 *Physica C* **173** 309
- [14] Loram J W, Mirza K A and Freeman P F 1990 *Physica C* **171** 243
- [15] Affronte M, Pavuna D, Francois M, Licci F, Besagni T and Cattani S 1989 *Physica C* **162–164** 1007
- [16] Zhao Y, Zhang H, Sun S F, Su Z P and Zhang Q R 1988 *Solid State Commun.* **67** 31
- [17] Jayaram B, Lanchester P C and Weller M T 1991 *Phys. Rev. B* **43** 5444
- [18] Maeda H, Koizumi A, Bamba N, Takayama-Muromachi E, Izumi F, Asano H, Shimizu K, Moriwaki H, Maruyama H, Kuroda Y and Yamazaki H 1990 *Physica C* **157** 483
- [19] Shaked H, Faber J Jr, Veal B W, Hitterman R L and Paulikas A P 1990 *Solid State Commun.* **75** 445
- [20] Dong K Le, Renard J P, Velu E and Lalar R 1989 *Solid State Commun.* **72** 89
- [21] Xu Y W, Sabatini R L, Moodenbaugh A R, Zhu Y, Shyu S G, Suenaga M, Dennis K W and McCallum R W 1990 *Physica C* **169** 205
- [22] Dou S X, Liu H K, Bourdillon A J, Savvides N, Zhou J P and Sorrell C C 1988 *Solid State Commun.* **68** 221
- [23] Westerholt K, Wuller H J, Bach H and Stauche P 1989 *Phys. Rev. B* **39** 11 680
- [24] Tome-Rosa C, Jakob G, Maul M, Walkenhorst A, Schmitt M, Wagner P, Przyszlupski P and Adrian H 1990 *Physica C* **171** 231
- [25] Kakihana M, Borjesson L and Eriksson 1989 *Physica C* **162–164** 1251
- [26] Roughani B, Sengupta L C, Auel J L and Sundaram S 1991 *Physica C* **171** 77
- [27] Zhao Y, Liu H K, Li J R, Yang G and Dou S X 1991 *Physica C* **185–189** 753

- [28] Altschuler B L, Khmel'nitski D, Larkin A I and Lee P A 1980 *Phys. Rev. B* **22** 5142
- [29] Meakawa S and Fukuyama H 1981 *J. Phys. Soc. Japan* **51** 1380
- [30] Batlogg B 1991 *Phys. Today* **44** 44
- [31] Zhao Y, Zhang H, Tang M Q and Zheng Q R 1990 *Prog. Phys.* **10** 421
- [32] Chien T R, Wang Z Z and Ong N P 1991 *Phys. Rev. Lett.* **67** 2088
- [33] Tinkham M 1975 *Introduction to Superconductivity* (New York: McGraw-Hill) ch 8
- [34] Marsiglio F 1992 *Phys. Rev. B* **45** 956